GEOPHYSICAL RESEARCH LETTERS, VOL. 36, L15206, doi:10.1029/2009GL038945, 2009

Click Here for Full Article

Is the Martian water table hidden from radar view?

W. M. Farrell,[1] J. J. Plaut,[2] S. A. Cummer,[3] D. A. Gurnett,[4] G. Picardi,[5] T. R. Watters,[6] and A. Safaeinili[2]

Received 29 April 2009; revised 3 June 2009; accepted 17 June 2009; published 14 August 2009.

[1] Mars may possess a global sub-surface groundwater table as an integral part of its current hydrological system. However, the Mars Advanced Radar for Subsurface and Ionospheric Sounding (MARSIS) onboard the Mars Express (MEx) spacecraft has yet to make a definitive detection of such a body of liquid water. In this work, we quantify the conditions that would allow a detection of a deep aquifer and demonstrate that the lack of radar detection does not uniquely rule out the presence of such a body. Specifically, if the overlying crustal material has a conductivity above $\sim 10^{-5}$ S/m (equivalent to a loss tanget of 0.008), a radar echo from an aquifer could be sufficiently attenuated by the intervening medium to prevent its detection by MARSIS. As such, the lack of direct detection by MARSIS–a "null result"–does not rule out the possibility of the water table's existence. **Citation:** Farrell, W. M., J. J. Plaut, S. A. Cummer, D. A. Gurnett, G. Picardi, T. R. Watters, and A. Safaeinili (2009), Is the Martian water table hidden from radar view?, *Geophys. Res. Lett.*, *36*, L15206, doi:10.1029/2009GL038945.

1. Introduction

[2] While it has been postulated that Mars' surface once contained large amounts of liquid water, what remains is a relatively small body of water-ice at each pole that, if fully melted, is the global equivalent layer of water of 10's of meters depth [*Smith et al.*, 2001; *Plaut et al.*, 2007]. Based on current surface conditions, if a large body of water existed, it is presumed to either have been lost via atmospheric escape or to fully/partially reside deep in the subsurface where crustal temperatures may support a liquid state [*Clifford*, 1993; *Clifford and Parker*, 2001]. The location of a subpermafrost groundwater table is presumed to be below the subsurface melting isotherm defined as the depth where geothermal heat flux through the thermally conductive crust maintains a temperature of 273K. *Clifford and Parker* [2001] estimate the depth to this melting isotherm to be <5 km at 30° latitude and <9 km at 60° latitude. Above this depth any water is presumably in the form of a solid, in a permanently frozen zone consisting of ice or an ice-soil mixture called the "cryosphere." The authors note that a specific set of assumptions are made to calculate the cryosphere thickness/melting isotherm depth that can only be verified via a future geophysical study. As such, there is considerable uncertainty on these values [*Clifford et al.*, 2009].

[3] One way to obtain information on the presence of a subsurface water table is with ground penetrating radar (GPR) at low frequencies that allow remote sensing of the subsurface. Since the water table aquifer will have a differing permittivity relative to the overlying rock, a radar reflection might be anticipated from this region. Low frequency radar allows for relatively deeper penetration into the overlying material and ice. MARSIS is such a ground-penetrating radar system that operates in 4 subsurface sounding bands between 1.3–5.5 MHz, each with a bandwidth of 1 MHz. Since antenna deployment in mid-year 2005, nearly the entire planet has been covered via MEx's highly inclined orbit. More details on the instrument are given by *Jordan et al.* [2009].

[4] In polar regions, the MARSIS radar signal was found to penetrate to the base ($\sim$3 kilometers) of both the northern and southern polar layer deposits (PLD) [*Picardi et al.*, 2005; *Plaut et al.*, 2007]. The attenuation in most regions of the PLD was surprisingly small at 4–5 MHz, suggesting that the layered deposits are relatively cold (below 240K) and low in impurities [*Picardi et al.*, 2005; *Plaut et al.*, 2007]. The region near Chasma Australe was specifically examined in detail for evidence of melting, and no obvious sub-surface aquifer was found [*Farrell et al.*, 2008]. However, there are "patchy" regions under the PLD lacking clear return echoes, called "amorphous regions." The lack of a coherent return signal creates an ambiguous situation in the search for basal lakes/interglacial aquifers (further described by *Farrell et al.* [2008]).

[5] In non-polar regions, there are a limited number of reports of MARSIS detections of subsurface stratigraphy, and these reports are associated with specific locations. *Picardi et al.* [2005] and *Watters et al.* [2006] found evidence of buried craters a few hundred kilometers in diameter and at depths of 1–2 km, with radar returns consistent with reflections from the crater walls and floor. However, *White et al.* [2009] suggest that a fraction of these signatures are due to apparent distortions of the surface echoes by the ionosphere, as opposed to a definitive subsurface structure. *Watters et al.* [2007] also detected a clear unambiguous subsurface interface in the Medusae Fossae Formation to a depth of 1–2 km. The top layer thickness varies with topography suggesting that a young deposit (volcanic ash, porous rock, or ice) is overlaid on top of the lowland plains. *White et al.* [2009] detected a subsurface linear interface from an apparent crater-filling deposit in the Ma'adim Vallis region. *Boisson et al.* [2009] used the signal absorption very close to the surface return

[1]NASA Goddard Space Flight Center, Greenbelt, Maryland, USA.
[2]NASA Jet Propulsion Laboratory, Pasadena, California, USA.
[3]Electrical and Computer Engineering Department, Duke University, Durham, North Carolina, USA.
[4]Department of Physics and Astronomy, University of Iowa, Iowa City, Iowa, USA.
[5]Infocom Department, La Sapienza, University of Rome, Rome, Italy.
[6]CEPS, NASM, Smithsonian Institution, Washington, D. C., USA.

0094-8276/09/2009GL038945$05.00

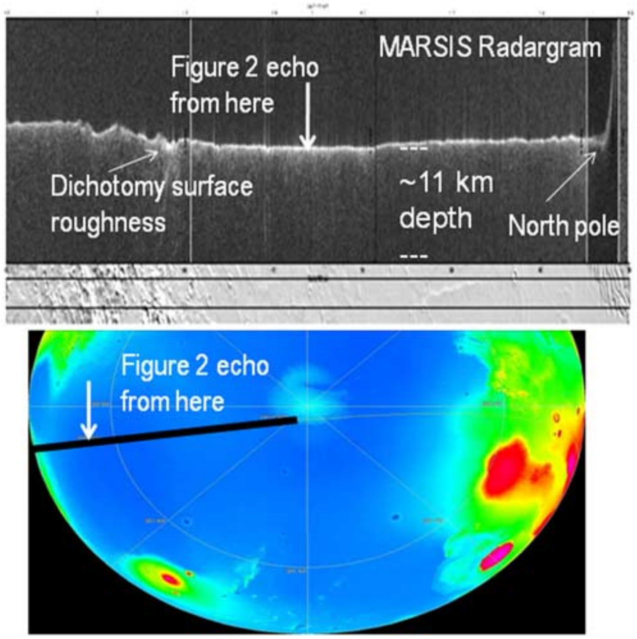

Figure 1. A MARSIS radargram from orbit 3869 and a map of the associated groundtrack. The spacecraft passes over the northern lowlands on the Martian nightside.

pulse to infer the presence of a 30–50-m thick volcanic layer on the Athabasca valley surface.

[6] However, to date, there is no report of an interface associated with a deeper groundwater table. Figure 1 (top) shows a MARSIS radargram with the radar echo delay plotted vertically as a function of Mars Express (MEx) sub-satellite position. Figure 1 (bottom) shows the associated MEx groundtrack over the northern lowland regions, this occurring during Martian nighttime. The periapsis is at $\sim 37^\circ$ latitude and the nighttime conditions allow penetration of the 4 MHz signals through the low-plasma-density nightside ionosphere [*Gurnett et al.*, 2005]. The radargram can be considered a cross section of the northern lowlands. The primary signal detected in the lowland region is the return pulse from the Martian surface. The radargram shows a complete absence of any subsurface return. A few apparent subsurface bright spots early in the pass result from surface clutter associated with the rougher terrain typically found at the dichotomy boundary. There is no evidence for a strong reflector deep under the surface.

[7] There are a number of scenarios to explain the radargram and the many others like it that show no evidence for a water table in the northern lowlands. First, the lack of detection could imply that there is no water table and that the subsurface is basically free of liquid water. In this case, the sub-surface temperature remains below freezing to at least the depth of the MARSIS sampling window ($\sim$11 km in depth assuming a relative dielectric permittivity of 6 for basalt), keeping water in ice form. The cold sub-surface also keeps the polar ice from melting, consistent with the lack of MARSIS detection of basal melting under the PLD. Alternatively, the subsurface may be essentially free of H_2O, liquid or solid. Another scenario is that the water table is there, but the intervening material is very lossy, thus attenuating any return signal from an aquifer to levels below the system noise level at the spacecraft. In this paper, we will investigate the conditions that might create this "lossy" situation. We want to determine the characteristics of the near-surface crustal material required to attenuate an aquifer return echo and hence "hide" any aquifer from view of the radar.

2. Return Echo: The Presence of a Long Tail

[8] Figure 2 shows a 20-second average of the overall signal return from the region near the 320 km periapsis altitude. The most distinct feature is the well-defined intensity peak of about 35 dB above the noise level as the 4 MHz signal pulse is reflected from the surface. This return echo is commonly called the "surface pulse." The noise level is defined as the power flux detected prior to the surface pulse, when no return echoes are in range (i.e., in the first 80 microseconds of Figure 2, prior to any echo return to MARSIS). This level is presumed to be representative of the cosmic background level at 4 MHz of $\sim 10^{-19}$ W/m^{2}Hz [*Dulk et al.*, 2001].

[9] An interesting observation is the long echo "tail" that continues for nearly 140 microseconds after the peak surface return pulse, with signal levels above the comic noise level. Comparison of this long echo to models of topographic surface clutter indicates that the extended echo is not associated with any sub-surface phenomena but instead is due to off-nadir clutter. Even though a northern lowland pass was chosen due to its relative smoothness, there is still enough off-nadir relief to give rise to an apparent ray time delay resulting from reflections from off-nadir rough terrain. This "long-tail" feature in the surface return echo is consistently observed throughout the pass in the lowland regions from the dichotomy boundary to the PLD near the end of the pass.

[10] To be detected, any water table in the subsurface has to have a return echo signal that exceeds the clutter-defined noise level in Figure 2. As such, the cosmic background level, like that observed in the first 80 microseconds of Figure 2, is not the fiduciary noise level of detection. The

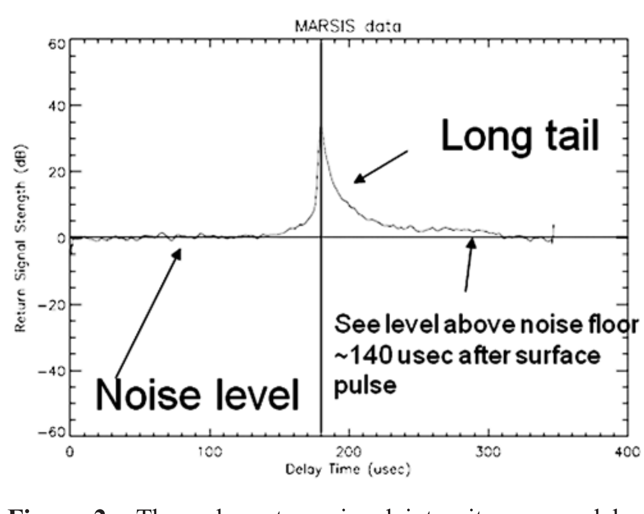

Figure 2. The radar return signal intensity versus delay time for a section of the northern lowlands (sampled region indicated in Figure 1).

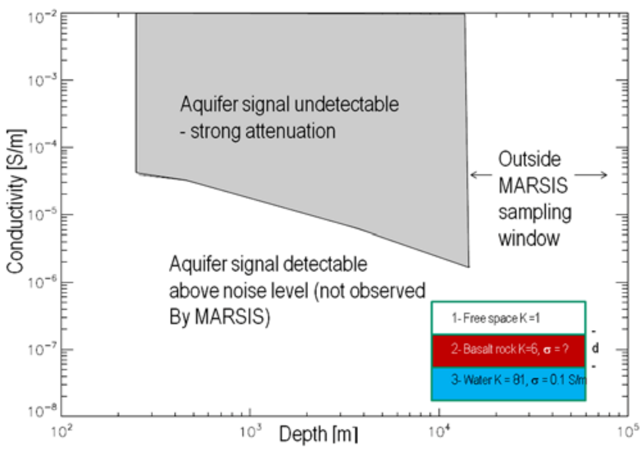

Figure 3. Aquifer detection as a function of overlying crustal material (soil/rock) conductivity and depth. Inset includes the configuration of the layering of the radio two-layer model; the reflection is from the top of the third layer that lies a distance d below the surface.

defining noise level required to be exceeded is instead the more intense clutter noise level, S_n [*Picardi et al.*, 2004].

3. Analytical Modeling

[11] In order to evaluate the effect of a lossy crustal material on groundwater table detection, we will assume that a water table/aquifer is indeed present, but that the overlying icy soil absorbs the radar signals, effectively "hiding" the aquifer from view. This situation requires that the crustal material attenuation be strong enough to reduce the aquifer echo power level to be just below the clutter-defined noise power flux level shown in Figure 2, $S_{aq} < S_n$. In order to quantify this effect, we apply a very simple two layer model (like that shown in the inset of Figure 3), where a radar signal in free-space (medium 1) enters a basaltic layer (medium 2) with a real permittivity, K_2, of $\sim$6 and unknown conductivity, σ_2. Medium 2 extends to a depth, d. The ray then reflects from the top surface of an aquifer (medium 3) with an assumed high reflectance of $R_{23} \sim 0.98$. In the model, we will attempt to constrain the values of σ_2. We can analytically define this situation as [*Eaves*, 1987; *Farrell et al.*, 2005]:

$$S_{aq} = G\ F(r')B \exp(-A) < S_n \tag{1}$$

where S_{aq} is the return aquifer power flux to MEx (in units of W/m^{2}Hz), S_n is the return pulse and associated clutter noise level shown in Figure 2, G is the MARSIS receiver processing gain (G is typically $\sim$30–40 dB [*Jordan et al.*, 2009]) applied to the chirp returns, F is the return power flux from a flat perfect reflector defined by *Calvert et al.* [1995] as $F(r) = P/(16\ \pi\ r^2\ \Delta f)$, where P is the MARSIS 4 MHz transmitted power of 5–10 W, r is the spacecraft distance to the surface (of about $\sim$320 km at periapsis), and Δf is the bandwidth of 1 MHz. We note that $r' = r + d$ where d is the depth from the surface to the aquifer (see inset of Figure 3). However, $r \gg d$ and for the calculations used here $F(r + d) \sim F(r)$. B is equal to $T_{12}^2 R_{23}$ and lumps the two power transmissions at the free-space/rock boundary (T_{12}) and the single power reflection at the rock/water boundary (R_{23}) into one variable having a value of about 0.65. The variable A is of primary interest - defining the attenuation of the medium. For relative permittivity K_2 greater than $\sigma_2/\omega\varepsilon_o$, we can write $A \sim 4\ n_i\ \omega\ d/c \sim 2\sigma_2 d/\varepsilon_o\ K_2^{1/2}c$, where n_i is the imaginary part of medium 2's index of refraction, ω is the wave frequency, ε_o is the permittivity of free space, c is the speed of light and σ_2 is the conductivity of the overlying material. As the conductivity of the overlying rock increases, attenuation of the deep aquifer return signal increases in a geometric fashion.

[12] The terms of equation (1) can be rearranged to arrive at a condition on the crustal conductivity consistent with $S_{aq} < S_n$, namely,

$$\sigma_2 > -(2d)^{-1}\varepsilon_o K_2^{1/2}\ c\ \ln(S_n/G\ F(r)B). \tag{2}$$

In essence, if the conductivity of the absorbing rock remains above the value derived by equation (2), then an aquifer will remain undetectable. We can now use the clutter-defined noise level in Figure 2 to estimate the lower limit of the conductivity in equation (2). Figure 2 shows the noise power flux $S_n = S_n(\Delta t(d))$, where Δt is the time separation between the surface return pulse and later times (or lower depths, $d = c\ \Delta t/2\ K_2^{1/2}$). As an example, if we assume an aquifer is located at 2.5 km depth, then the return signal delay relative to the peak of the surface return pulse is Δt of 42 microseconds, and $S_n(\Delta t = 42\ \mu\text{sec})$ is $\sim$4 dB above the cosmic background noise level of $\sim 10^{-19}$ W/m^{2}Hz [*Dulk et al.*, 2001].

[13] There are two methods for obtaining the gain factor, G. First, it can simply be set to 35 dB based on previous analysis/knowledge [*Jordan et al.*, 2009]. Since the value resides in the natural-log term, large variations of the value (10's of percent) will not greatly alter the overall result. However, a second method allows a value that is consistent with the modeling, by comparing the actual return surface pulse peak in Figure 2 to that theoretically expected from a free-space/basalt interface. A return surface echo has a power flux that is defined by

$$S_{peak} = G\ F(r)R_{12} \tag{3}$$

where R_{12} is the reflectance from the free-space/basalt interface (and is $\sim$0.17 for $K_2 \sim 6$). The derived value of F is approximately 10^{-18} W/m^{2}Hz at an altitude of 320 km, and S_{peak} is the observed peak value of the surface return signal in Figure 2 following the inclusion of processing gain, G, at $\sim 3 \times 10^{-16}$ W/m^{2}Hz. Hence, G approximately equals $S_{peak}/F(r)R_{12}$ and is about 1860 (or $\sim$33 dB) during this period.

[14] We now have all the information required to solve equation (2) for σ_2. Figure 3 shows the conductivity ranges that both allow and disallow water table detection. Note that for crustal conductivity above about $\sim 10^{-5}$ S/m (equivalent to a loss tangent of >0.008), a deep aquifer could in fact be hidden from MARSIS. If the crustal conductivity is below 10^{-5} S/m, an aquifer return pulse would not be absorbed by the surrounding medium and might possibly have been observed by MARSIS, if it exists.

[15] Note that the limiting conductivity varies as ln (S_n/G F(r) B) and thus changes in parameters by factors of 10 alter

the conductivity by only small factors. While a more sophisticated model might including scattering from smaller intervening layers (dielectric contrast), there is no evidence for the existence of such layers in the radargram in Figure 1. Further, *Farrell et al.* [2005] produced such a model for PLD application (using MOC-observed layering structure) and found that scattering from dielectric contrast attenuated the return signal by only a factor of 2. Again, given that such a factor would be folded within the natural log function in equation (2), the inclusion of similar scattering from such layering would be artificial (contrived) and in the end would not substantially alter the result. In other words, a more sophisticated model is not required to demonstrate the inherent lack of uniqueness in the non-detection.

[16] Finally, by inverting equation (2), we find that the transmitter power required to detect an aquifer at 10 km depth varies as $P = \beta \exp(\sigma/\alpha)$ where $\alpha = (2d)^{-1}\, \varepsilon_o\, K_2^{1/2}\, c \sim 3.2 \times 10^{-7}$ S/m and $\beta = 5W\, S_n(d = 10\text{ km})/G\, F(r)\, B \sim 5 \times 10^{-4}$ W, where the value of 5W is the MARSIS transmitter power that is used as a reference point for scaling. At $\sigma = 3 \times 10^{-6}$ S/m, P is $\sim$5W, consistent with Figure 3. However, if the overlying medium has a substantially higher conductivity, the required transmission power becomes very large, beyond the capabilities of modern space-based radars. For example, if the overlying conductivity of the medium of $\sigma = 6 \times 10^{-6}$ S/m, the required transmission power to detect the aquifer at a 10 km depth is now nearly 70 kW.

4. Conclusions

[17] We find that if the Martian northern lowlands has a overlying crustal material with a bulk conductivity of $>10^{-5}$ S/m (loss tangent > 0.008), detection of an echo from subpermafrost groundwater table in the top 11 km of the subsurface will become problematic due to attenuation in the overlying rock. The conductivity of permafrost itself ranges from 10^{-5} to 10^{-2} S/m [*Daniels*, 1996] and an extended layer of hardened icy rock could account for the signal loss – but this inference is non-unique. As such, the lack of an observed groundwater table detection by MARSIS, the "null result" shown in Figure 1, does not automatically rule out the possibility of the water table's existence.

[18] In arriving at this result, there are numerous assumptions being made, including that the boundary between the rock and water is relatively sharp and distinct, giving rise to an easily calculated reflectance. We make the ideal assumption that the water table reflectance is a large value (nearly unity), thus allowing us to easily attribute the calculated losses to the overlying medium. In reality, the transition from ice-filled porous rock into liquid water-filled rock of the groundwater table may not be sharp and distinct on the scale-size of a wavelength, effectively reducing the reflectance from the high value assumed. Thus, in Figure 3, for a factor of 10 reduction from the assumed reflectance (now $R_{23} \sim 0.1$), the bottom of the shaded region is downward shifted in conductivity by a factor of $\ln(10) \sim 2.3$, and for $R_{23} \sim 0.01$, this boundary line is downshifted in conductivity by a factor of $\ln(100) \sim 4.6$. Again, large changes in assumed reflectance create only a mild shift in the result.

[19] Another assumption is that the water table lies within the 11 km region sampled. A recent reexamination of the heat flux suggests that indeed the table may be lower in depth than previously predicted [*Clifford et al.*, 2009]. We thus limit our conclusions to a depth of $D = cT/2n \sim 11$ km, where T is approximately $^1/_2$ the MARSIS detection window of ($\sim$180 microseconds). If the water table lies below the MARSIS detection window of $\sim$11 km, then even a strong return signal is delayed for such a long time as to be missed by MARSIS. We do not consider herein magnetic losses [*Stillman and Olhoeft*, 2004] which may further attenuate the signal in the rocks.

[20] Despite these assumptions, the inversion of the null result into a bounding estimate of the sub-surface conductivity has its own merits. At the very least, the limit is a starting point for the design of Martian GPRs that may fly on future rovers/landers. Specifically, such GPRs may require high powers to overcome an inherently lossy medium to obtain a deep groundwater table signature. We especially note herein that our bound is a lower limit, and the conductivity may be substantially higher than the $\sim 10^{-5}$ S/m derived via inversion of the system noise level.

References

Boisson, J., et al. (2009), Sounding the subsurface of Athabasca Valles using MARSIS radar data: Exploring the volcanic and fluvial hypotheses for the origin of the rafted-plate terrain, *J. Geophys. Res.*, doi:10.1029/2008JE003299, in press.

Calvert, W., et al. (1995), The feasibility of radio sounding in the magnetosphere, *Radio Sci.*, *30*, 1577, doi:10.1029/95RS01731.

Clifford, S. M. (1993), A model for the hydrologic and climatic behavior of water on Mars, *J. Geophys. Res.*, *98*, 10,973, doi:10.1029/93JE00225.

Clifford, S. M., and T. J. Parker (2001), The evolution of the Martian hydrosphere: Implications for the fate of a primordial ocean and the current state of the northern plains, *Icarus*, *154*, 40, doi:10.1006/icar.2001.6671.

Clifford, S. M., et al. (2009), The occurrence and depth of subpermafrost groundwater on present-day Mars: Implications of revised estimates of crustal heat flow, thermal conductivity, and freezing point depression, *Lunar Planet. Sci. Conf.*, *XL*, Abstract 2557.

Daniels, D. J. (1996), *Surface-Penetrating Radar*, *IEE Radar Sonar Navig. Avionics Ser.* vol. 6, Inst. of Electr. and Electr. Eng., London.

Dulk, G. A., et al. (2001), Calibration of low frequency radio telescopes using the galactic background radiation, *Astron. Astrophys.*, *365*, 294, doi:10.1051/0004-6361:20000006.

Eaves, J. L. (1987), Introduction to radar, in *Principles of Modern Radar* edited by J. L. Eaves and E. K. Reedy pp. 1–27, Van Nostrand Reinhold, New York.

Farrell, W. M., J. J. Plaut, D. A. Gurnett, and G. Picardi (2005), Detecting sub-glacial aquifers in the north polar layered deposits with Mars Express/MARSIS, *Geophys. Res. Lett.*, *32*, L11204, doi:10.1029/2005GL022488.

Farrell, W. M., et al. (2008), MARSIS subsurface radar investigations of the south polar reentrant Chasma Australe, *J. Geophys. Res.*, *113*, E04002, doi:10.1029/2007JE002974.

Gurnett, D. A., et al. (2005), Radar sounding of the ionosphere of Mars, *Science*, *310*, 1929, doi:10.1126/science.1121868.

Jordan, R., et al. (2009), The Mars Express MARSIS Sounder Instrument, *Planet. Space Sci.*, (submitted).

Picardi, G., et al. (2004), Performance and surface scattering models of Mars Advanced Radar for Subsurface and Ionosphere Sounding (MARSIS), *Planet. Space Sci.*, *52*, 149, doi:10.1016/j.pss.2003.08.020.

Picardi, G., et al. (2005), Radar soundings of the subsurface of Mars, *Science*, *310*, 1925, doi:10.1126/science.1122165.

Plaut, J. J., et al. (2007), Subsurface radar sounding of the south polar layered deposits on Mars, *Science*, *316*, 92, doi:10.1126/science.1139672.

Smith, D. E., et al. (2001), Mars Orbiter Laser Altimeter: Experiment summary after the first year of global mapping of Mars, *J. Geophys. Res.*, *106*, 23,689, doi:10.1029/2000JE001364.

Stillman, D. E., and G. R. Olhoeft (2004), GPR and magnetic minerals at Mars temperatures, paper presented at 10th International Conference on GPR, Delft, Netherlands.

Watters, T. R., et al. (2006), MARSIS radar sounder evidence of buried basins in the northern lowlands of Mars, *Nature*, *444*, 905, doi:10.1038/nature05356.

Watters, T. R., et al. (2007), Radar sounding of the Medusea Fossea Formation of Mars: Equatorial dry ice or dry, low density deposit?, *Science*, *318*, 1125, doi:10.1126/science.1148112.

White, O., et al. (2009), MARSIS radar sounder observations in the vicinity of Ma'adim Vallis, Mars, *Icarus*, *201*, 460, doi:10.1016/j.icarus.2009.01.015.

S. A. Cummer, Electrical and Computer Engineering Department, Duke University, Durham, NC 27708, USA.

W. M. Farrell, NASA Goddard Space Flight Center, Code 695, Greenbelt, MD 20771, USA. (william.m.farrell@gsfc.nasa.gov)

D. A. Gurnett, Department of Physics and Astronomy, University of Iowa, Iowa City, IA 52242-1479, USA.

G. Picardi, Infocom Department, La Sapienza, University of Rome, I-00184 Rome, Italy.

J. J. Plaut and A. Safaeinili, NASA Jet Propulsion Laboratory, MS 183-501, Pasadena, CA 91109, USA.

T. R. Watters, CEPS, NASM, Smithsonian Institution, Washington, DC, 20560-0315 USA.